

A NONDIRECTIONAL INFRARED TRANSCEIVER FOR INDOOR HIGH SPEED WIRELESS DATA COMMUNICATION*

Tay-Her Tsaur[†], Kwang-Cheng Chen[†], Member, IEEE, Chenhsin Lien[†], Ming-Tang Shih[‡],
C. P. Jeremy Tzeng[‡], Senior Member, IEEE

Abstract

A prototype of the 1M bps non-directive infrared wireless transmission system was designed, and tested. System design considerations about channel property, optoelectronics devices characteristics, modulation schemes are discussed, and issues about the circuit design and the implementation are described. In this system, the pulse position modulation (PPM) with short pulse duration and the analog-multiplier type demodulator were used. The feasibility of nondirective transmission is fully demonstrated and can support successful data communication in a typical room. The system architecture can be upgraded to data rates such as 2M bps or higher by only changing circuit parameters.

I. Introduction

In the past few years, the growth of computer-based terminal stations, such as PCs, workstations, etc., was enormous. Subnotebook PCs, portable workstations are currently available with small size and high performance. Merging with another tremendous trend in networking, the need of the data communication for these terminals is for sure. Traditional data communication is achieved by wired physical connection, such as twist-pair lines, coaxial cables, or optical fibers. These physical "wires" introduce difficulties in construction and rewiring during system setting up, maintenance, and expansion. The rapid growth in portable stations and their necessity in mobile data communication services makes conventional network unsatisfactory.

An alternative to achieve the same goal for portable stations is the wireless network. The troubles and the cost due to wires also can be reduced or eliminated in the wireless systems. Traditionally, radio-frequency transmission was used in wireless applications. However, the spectrum is so crowded that it is very difficult (if not impossible) to get permis-

*This research was supported by the Computer and Communication Laboratory, Industrial Technology Research Institute, Hsinchu, Taiwan, R.O.C.

[†]The authors are with the Department of Electrical Engineering, National Tsing Hua University, Hsinchu, Taiwan 30043, R.O.C.

[‡]The authors are with the Computer and Communication Laboratory, Industrial Technology Research Institute, Hsinchu, Taiwan, R.O.C.

sion for these new high rate applications. Optical systems with low implementation complexity and no spectrum license requirement are providing a possible solution. Researchers at the IBM Zurich Laboratory [1] pioneered the feasibility of a baseband 125K bps transmission via diffuse infrared radiation. Similar efforts have been continued [2-6] since then. In this paper, we will demonstrate a 1M bps non-directive transmission prototype for data communication, and discuss issues in designing and implementation. This paper is organized as follows. In Section II, we describe issues about non-directive optical channel, optoelectronics device limitations, and our solutions in modulation methods and system designs. In Section III, the implementation techniques of all subsystems in our prototype are described. Experimental results and conclusion are arranged in Section IV and V.

II. System Design

The block diagram of our transceiver design is shown in Figure 1. The transmitter part includes a parallel-to-serial interface, a modulator, a power boosting stage, and some electroluminescence devices. The receiver part contains photodetector, a low noise amplifier, a demodulator, clock recovery circuit, and some interfaces for output. To achieve 1M bps transmission rate, the design on each subsystem is described in the following sections.

A. Channel Property and Optoelectronics Devices Characteristic in Nondirective Optical Channel

For a nondirective optical communication system, the system performance strongly depends on the illumination over the photodetector [4]. Some early research by Gfeller and Mandai described the optical spectral power density and the interference signal frequency of the indoor illumination. For filament lamp, the wavelength of maximum spectral power density is about $1 \mu\text{m}$. Most optical power of the fluorescent lamp is emitted in the visible light range (wavelength less than $0.8 \mu\text{m}$) which depends on the type of lamp [7]. For sunlight, the maximum of the power spectral density is located at about $0.5 \mu\text{m}$ with very wide bandwidth. However, because the photodetector is not sensitive only to a particular wavelength only, all effects of light sources to photodetector should be taken into consideration. In our prototype, we used

silicon PIN photodiode with 10 pF capacitance and 3.23 mm^2 active area reverse-biased at -10 V . Since the Si PIN photodiode is inexpensive, widely available in the market, and well behaved in the near-infrared spectral range (wavelength less than $1.1 \mu\text{m}$) [8], thus it is adopted here. The fluorescent lamp will generate $0.25 \mu\text{App}/\text{mm}^2$, 120 Hz photocurrent with little dc component by setting four 40W fluorescent lamps 2m away from the photodiode. For filament lamps, the measured photocurrent was $0.5 \mu\text{App}/\text{mm}^2$, 120 Hz with $2.5 \mu\text{A}/\text{mm}^2$ dc offset by a 60W bulb 0.5m away from the photodetector. In addition, with a thyristor dimmer, the filament lamp generated sharp spike at a period of $1/120 \text{ sec}$ and high frequency harmonics will be generated. For inverter fluorescent lamps (13W, 0.5m to the photodiode), the measured photocurrent was $30 \text{ nApp}/\text{mm}^2$, 55 KHz with $0.22 \mu\text{A}/\text{mm}^2$ dc offset. In our experiment, we noticed that the EMI from this lamp was quite large. Some interferences still can be observed even if the photodiode has been removed. The effect of sunlight can be considered as a dc offset and most of its power is located in the visible light range. Thus, it is far less important than other sources of interference and can be negligible here.

The measurement of indoor illumination sources shows that most of the interferences are in the low frequency range except for inverter fluorescent lamps. Therefore, it is beneficial to arrange signal power in high frequency range such that the low frequency interference can be filtered out by a high pass filter. For the inverter fluorescent lamp, this method will not work well because the interference frequency is very high. From the viewpoint of the spectrum of the light source, an optical band pass filter can effectively reduce the high frequency interference [9]. For fluorescent lamps and inverter fluorescent lamps, most of their emitted light power is located in the visible spectral range and the optical band pass filter will work very well. For filament lamps, quite large amount of their emitted power is in the near-infrared range, thus the optical band pass filter can not remove this kind of interference.

We chose the silicon PIN photodiode as the photodetector for both initial experiment and final implementation because it has very good responsivity for wavelength only up to $1.1 \mu\text{m}$. Since the current gain of the avalanche photodiode (APD) is highly nonlinear and very sensitive to the reverse bias voltage [10], thus its current gain will be strongly modulated by the interference from the indoor illumination. This will greatly distort the received signal and make the APD undesirable for the simple nondirective optical communication.

The LED and laser diode (LD) are two available sources for the optical communication. Since the required transmission power in the nondirective optical communication is usually far beyond the limit of a single device, a multi-device array is needed. It is preferred to use LED here by taking advantages of its simple driver circuit and lower price. However, LD can be used either the price of the LD and its driver is low enough or the high speed is required.

The drawbacks of the LED are its relative low operation speed and low efficiency [11]. A technique which is widely used in infrared remote control system can raise the peak output power of LED. In this technique, LED is driven by short pulse with high peak value current. However, the use of this operation mode is quite limited from the modulation scheme point of view.

Directivity of the light source and the photodetector is very important parameter in nondirective optical communication. Wide field of view (FOV) is highly preferred to build up a robust system. The FOV can be enlarged either by using a diffusion lens or by using an array of LEDs together with an array of photodetectors. At the transmitter end, we used an LED array to satisfy both FOV and power requirements. Diffusion lens were not used in our system due to their high cost and relatively low performance gain.

B. Modulation Method

The LED was used as the light source in our system. Considering the choice of the modulation method, we should note the speed limitation of LED and the use of short pulse operation. According to earlier study [4], the short pulse operation are good for diffused infrared system. We use infrared LED with 12 MHz bandwidth in our system. In short pulse operation, the bandwidth would be further reduced due to the deep saturation and the charge time for stray capacitance, thus we only take baseband transmission schemes into consideration. In addition, we also try not to generate carrier to save the power. To filter out the $1/f$ noise and the 60Hz interference which are the most troublesome interference sources for such baseband communication system, modulation methods with less low-frequency power are preferred.

Among many modulation methods used in baseband transmission which are different in signal bandwidth, clock term existence, dc term transmission requirement, etc. [12]. practical limitations in nondirective optical channel make some of them inadequate. Since undesired low frequency terms will be removed, those methods requiring dc term to carry information can not be used.

Multipath effect is another serious problem in the nondirective optical communication. Multi-reflection in normal office environment may cause intersymbol interference. Some early research result points out this will strongly depend on the modulation schemes. However, for a 1 MHz bps system, multi-path transmission is not a serious problem [4].

Following traditional economical direct detect modulation, two methods for non-directive optical communication, on off keying (OOK) and pulse position modulation (PPM) were studied earlier [4],[5],[13]. As the conclusion of [4],[5],[13], we select binary PPM (also known as Manchester code) in our system implementation due to its inherent clock information buried in symbol sequence. For PPM, pulse width and pulse position will affect transmission signal spectrum distribution. For narrow pulses,

in addition to a more robustness to the multipath effect, the transmission power will move up to the higher frequency range such that less power is within the range of indoor illumination interferences. The pulse width is limited by the switching characteristics of available LEDs. However, the bandwidth of pre-amplifier at the receiver end is finite and the intrinsic thermal noise also exists. Shorter pulse width may not always improve the system overall performance.

Pulse position will also affect power spectral distribution, especially in peak and null frequency. In our system we choose pulse position on "+/-90 degrees" position, that is, lagging or leading 250ns for digital "1" or "0". This choice will eliminate 1 MHz clock signal and together with its odd harmonics and leave its even harmonics. From the simulations with the pseudo-random input signal, we observe that there exists a strong and steady 2 MHz component which can be used for the clock recovery circuit and the demodulator. Pulse duration is chosen as 200 ns plus 100ns risetime and 100 ns falltime for further simulation, design, and prototyping. High value peak current on LEDs was used to increase the peak output power.

C. Overall system design

After the modulation scheme was decided, the block diagram of our system design is shown in Figure 2. The purpose of the system design is to build up a frame structure for the 1M bps system and the future expansion ability to higher speed operation. At the transmitter end, the PPM signal is generated with the NRZ signal and the clock signal. A duration controller is used for adjusting the pulse width and its output is fed to LED driver for the transmission. At the receiver, optical signal is converted to electrical signal by the photodetector. Its amplitude is amplified and properly controlled by automatic gain control (AGC) circuit. A phase-locked loop (PLL) is used to recover the clock signal for the demodulation. Demodulator together with some control logic circuit generates the original NRZ signal from received PPM signal. Please note that the AGC and the PLL are not necessary at low to moderate speeds operation. We include them here to ensure the robust performance.

III. Implementation Techniques

A. Preamplifier and Post-amplifier Design Consideration

Since indoor illumination interference is quite large in nondirective optical communication, the front end of the preamplifier should be able to handle large interference signal without losing linearity. The pre-amplifier would typically be able to handle 10 μ A dc term, 2000 nApp 120 Hz term and 100 nApp in 55 KHz interference. This makes the pre-amplifier in nondirective optical communication different from the pre-amplifier in optical fiber communication, where interference is typically not significant.

PIN diode photodetector has a depletion capacitance Cd in tens of pF order. For high speed operation the input impedance of pre-amplifier should be kept low. A transimpedance amplifier with negative feedback (NFB) [14] is used to achieve the low input impedance in the optical fiber communication. However, it is difficult to use the NFB without introducing the intermodulation distortion when there is a strong interference noise. Consequently, we use a common-base configuration followed by a cascode configuration as a compromise among the large dynamic range, the wide bandwidth, and the low thermal intrinsic noise in the pre-amplifier design. From the PSPICE simulation, the equivalent input thermal noise current spectral density is $1.7 \times 10^{-12} \text{ Arms}/\text{Hz}^{1/2}$ for pre-amplifier.

In our system, post-amplifier is just a driving stage with enough gain. A cascode stage followed by an emitter follower are used in the post-amplifier design. The shielding and the on board voltage regulator are necessary to prevent all stages of the amplifier from other interferences. De-coupling capacitors and resistors in each stage are also used to prevent the interference with other stage and the parasitic oscillation.

For transmission between portable stations and base stations, signal level is a strong function of the distance and the existence of the direct path. For proper clock recovery and demodulation, automatic gain control (AGC) is very helpful. In our design, we used a MOSFET as an attenuator to suppress the strong signal. A high speed level detector [15] and an amplifier with offset output voltage are used to generate the AGC control voltage. The MOSFET is an effective attenuator with over 30dB attenuation capability while introducing very little thermal noise current.

B. Gain budget

In this system design, the gain budget is estimated after the equivalent input noise current of the pre-amplifier has been figured out due to the limitation of the pre-amplifier. From the PSPICE simulations, we know that the equivalent thermal noise current spectral density is $1.7 \times 10^{-12} \text{ Arms}/\text{Hz}^{1/2}$, and from the data sheet we know the equivalent noise current spectral density of PIN diode is $1 \times 10^{-13} \text{ Arms}/\text{Hz}^{1/2}$, which can be ignored. If system bandwidth is 5 MHz, the equivalent input current noise would be 3.8 nA (rms). Assume that the overall transmission efficiency ζ from the LED driving current to the PIN diode photocurrent is 0.05 and the distribution of emitting light is uniform in semi-sphere. The distance of transmission is assumed to be 3 m, which is enough for a typical office. We would need an effective current of 1.33 A (rms) in driving LED in order to generate signal current equal to the internal noise current of the PIN photodiode. That is, 7.98 App (crest factor for PPM is 6) is needed to drive LED. Twenty LEDs will be needed if the peak current of the LED is less than 400 mA. For large PIN diode with 20.3 mm^2 active area, the require number of LEDs will be reduced to six. In our system we use

five LEDs due to the limitation of the driver.

For further processing in the receiver, the output of post-amplifier should be hundreds of millivolts. Hence the required overall transimpedance of amplifier would be about $1 \times 10^6 \Omega$ for 100 mVpp output while the signal current is about 4.4 times of the simulated equivalent input current noise. The low overall transmission efficiency ζ is due to the quite low efficiency of the LED. A further measurement showed that ζ was only 0.0266. A light source with higher efficiency will greatly enhance the overall system performance.

C. LED driver and Modulator

To generate PPM light pulses with the LED, a high speed and high current driver circuit is required. To design such a circuit, detailed knowledge of the LED characteristics and the large signal behavior of active devices are essential.

Basically, the LED is a PN junction and there exists delay and time constant between input electrical signal and output light power [11]. Thus we must use a high speed LED and a fast driving circuit with short delay time. In our circuit, we use push-pull driver to charge and to discharge LEDs promptly. Since the current would reach 500 mA level, care should be taken to reduce all time delays due to transistor drivers.

From the simulations, we learned that a steady usable 2 MHz component would exist if we put pulses at points of $+/- 90$ degrees. In later system design, this 2 MHz component was found to be very useful because we can generate and recover PPM signal based on system using this 2 MHz clock signal.

From a 2 MHz local quartz reference, we generate a 2 MHz signal. The 1 MHz signal as clock for the bit-flow and the 125 KHz clock for the byte-flow can be generated from a divided-by-16 binary counter. In each bit period, we can get 4 sections by logical combination of the 2 MHz clock and the 1 MHz clock. The spacing between two neighboring sections is 250 nS and the transitions just occurred at points of $+/- 90$ degrees. By logical combining the NRZ data signal and these transitions as trigger signals of one-shot circuit, we can generate the desired PPM signal and their pulse duration can be controlled by period of one-shot circuit. The whole process was done by TTL logic circuits. The concept and the implementation of this PPM signal generating circuit is quite simple. The operation of these circuits is shown in Figure 3.

D. Demodulator and Clock recovery

The basic concept of the binary PPM demodulator is to compare power between first half and last half in each bit period. This can be shown to be robust optimal in Gaussian noise that is generally true for our case. The performance of the simple level detection circuit would become unsatisfactory for the low SNR cases at higher rates.

A V-I converter and a load integral capacitor are key components in the demodulator. The block dia-

gram of the demodulator is shown in Figure 4. The received signal is first analog-multiplied with the recovered 1 MHz clock signal. If the received pulse is located in the positive period of the clock cycle, then it will remain as a positive pulse. As for the pulse located in the negative period of the clock cycle, it will be converted to a negative pulse. These processed signal pulses will be integrated on a capacitor, and each bit can be identified by its voltage polarity of the load integral capacitor. The capacitor is discharged for one bit period at the end of each bit. Two sets of this type demodulators operate in parallel to demodulate PPM signal in turn.

Some TTL circuits are used to generate all required control signal in the demodulator. Because the 2 MHz clock, a harmonic of bit rate, is used in this system, a problem that we can not distinguish continuous data string of "1" from continuous data string of "0" arises. We use a continuous data string of "0" as preamble and a detector for continuous string of "1" to solve this problem. Since transmitted data contains no continuous data string of "1", the system clock will be delayed by $0.5 \mu s$ for synchronization if a continuous data string of "1" is received.

For PPM signal used in our system, the 2 MHz clock is chosen as the main clock signal because of its availability. We used phase-locked loop (PLL) circuit with a front 2 MHz band pass filter for clock recovery in our system. The band pass filter is constructed by inductors, capacitors with trimmer, and a buffer stage to keep the bandwidth narrow.

A Gilbert-multiplier is used as the phase detector (PD) because of the received PPM signal may be greatly distorted. We use multivibrator-type voltage controlled oscillator (VCO) to make the acquisition fast because of its large gain and its wide frequency response range. Please note that the free run frequency of the VCO may cause the drift problem due to the variation of the ambient temperature or the power supply voltage. The loop filter is designed to have a 50 KHz bandwidth as the tolerance for the drift in the VCO, and a high dc gain for lower steady-state phase error. The lock-in range is dominated by this 50 KHz pole in our circuits. Because the free run frequency deviation of the VCO is usually much less than 50 KHz, the acquisition circuit is very fast.

IV. Experimental Results

In our circuit, a PPM signal with 80 ns rise-time, 200 ns at peak value, and 40 ns fall-time is achieved for driving LEDs with 358 mA peak current value. The transimpedance of our pre-amplifier is $1.7 \times 10^6 \Omega$ and its 3dB bandwidth is from 100 KHz to 8.5 MHz without PIN photodiode. As the transmission distance changed from 4.1m to 0.49m, the output of the amplifier changed from 180 mVpp to 270 mVpp. Signal can still be observed even without any direct paths. The bit error rate is about 10^{-7} to 10^{-5} , which depends on the strength of indoor illumination and the existence of the diffuse channel. For a smaller room, the received signal via multi-reflection is stronger. Thus, the transmission is more non-

directive and the bit error rate is lower. Please note that the intersymbol interference due to the multipath effect is not a problem in our system because of the short pulse width. Under the illumination of fluorescent lamps, the bit error rate is 3.8×10^{-5} in a large room where diffuse transmission is barely possible and the distance between the transmitter and the receiver is 1.2 m. The output waveform (upper trace) of the LED driver circuit which is a continuous train of "1" is displayed along with the received waveform (bottom trace) from the output of the preamplifier on figure 5. It is clear that both the LED driver circuit and the infrared sensing circuit performed excellently at 1 MHz operating frequency. The received waveform (upper trace) from the output of the preamplifier is displayed along with the output waveform from the demodulator (bottom trace) on figure 6. It is evident that the demodulator faithfully recovers the data train "10101100" sent from the transmitter. The photograph of the complete nondirective infrared transceiver with the transmitter on the left and the receiver on the right is shown on figure 7.

V. Conclusions

We demonstrate the feasibility of non-directive infrared wireless transmission through PPM scheme. From our experiment, we can observe that even there is no directive path, output signal of pre-amplifier is still visible and clear when the distance between the transmitter and the receiver is about 2 to 5 m, depending on the type of rooms. Besides, transmission through reflection by the ceiling or by the wall is also observed. At the 1M bps level, our system is a little bit overdesigned. However, such an architecture is aiming at higher speed. We successfully did a simple demonstration to upgrade the system into a 2M bps one based on the same system architecture. Therefore, we conclude that a system structure with a workable prototype justification toward 1M bps and higher speed nondirective in-room optical wireless data communication was designed successfully.

References

- [1] F. Gfeller, U. Bapst, "Wireless In-House Data Communication via Diffused Infrared Radiation", *IEEE Proceeding*, vol.67, no.11, pp.1471-1486, Nov. 1979.
- [2] T. S. Chu, M. J. Gans, "High Speed Infrared Local Wireless communications", *IEEE communications*, vol.25, no.8, pp.1-10, Aug. 1987.
- [3] C. S. Yen, R. D. Crawford, "The Use of Directed Optical Beams in Wireless Computer Communication", *Proceeding of Globecom'85*, pp.1181-1184, 1985.
- [4] K. C. Chen, "On Off Keying Optical Transmission and Channel Capacity for Indoor Wireless High Rate Wireless Data Networks", *Proc. IEEE Globecom'92*, pp.13.1.1-5, Phoenix, 1992.
- [5] K. C. Chen, et al., "Indoor High Speed Wireless Networks via Optical Transmission", *Records of the International Telecommunication Union Telecom'91 Technical Forum*, vol.2, pp.211-215, 1991.
- [6] J. Barry, J. Kahn, E. Lee, D. Messerschmitt, "High Speed Nondirective Optical Communication for Wireless Networks", *IEEE Communications*, vol.5, no.6, pp.44-54, Nov. 1991.
- [7] A. G. Jack, L. E. Vrenken, "Fluorescent Lamps and Low-Pressure Sodium Lamps", *IEE Proceeding Pt. A*, vol.127, No.3, pp.149-157, 1980.
- [8] J. Wilson, J. F. B. Hawkes, *Optoelectronics, an Introduction*, 2nd ed., U.K.: Prentice Hall International Ltd., 1989, p275.
- [9] K. Mandai, K. Miyauchi, M. Sugimoto, Y. Natsume, K. Ookubo, "An Advance Infrared Remote Control Sensor", *IEEE Transactions on Consumer Electronics*, vol.36, No.3, Aug. 1990, pp.669-677.
- [10] S. M. Sze, *Physics of Semiconductor Devices*, 2nd ed., Singapore: John Wiley and Sons, Inc., 1981, p686-p688.
- [11] A. Descombes, W. Guggenbuhl, "Large Signal Circuit Model for LED's Used in Optical Communication", *IEEE Transactions on Electron Devices*, vol.ED-28, No.4, Apr. 1981, pp395-404.
- [12] Hewlett-Packard Company, *Optoelectronics and Fiber-optics Applications Manual*, 2nd ed., p10.13-10.16.
- [13] K. C. Chen, C. H. Lee, "Capture in Multiple Access Lightwave Networks Employing Direct Detect Modulations", *Proc. IEEE Globecom'92*, Orlando, 1992.
- [14] J. Wilson, J. F. B. Hawkes, *Optoelectronics, an Introduction*, 2nd ed., U.K.: Prentice Hall International Ltd., 1989, p387-390.
- [15] K. F. Knott, "Sensitive Wideband Linear A.C.-D.C. Converter", *Proceedings of IEE*, vol.122, No.3, Mar. 1975, pp249-pp252.

Tay-Her Tsaaur received his B.S. in electrical engineering from the National Tsing Hua University, Hsinchu, Taiwan, in 1992. He is currently working toward his Ph.D. degree in the Semiconductor Technology and Application Research center (STAR) at the Department of Electrical Engineering, National Tsing Hua University. His current research interests include wireless data communication and integrated circuit design.

Kwang-Cheng Chen received the B.S. from the National Taiwan University, Taipei, Taiwan, in 1983,

and the M.S., Ph.D from the University of Maryland, College Park, Maryland, in 1987 and 1989 respectively, all in electrical engineering.

From 1983 to 1985, he taught telecommunication courses for military service in Taiwan. During 1985-1987 and 1988, he was a research assistant of System Research Center and Electrical Engineering Department at the University of Maryland, College Park. He participated in various VSAT system/network design projects with the Satellite Systems Engineering Inc., Bethesda, Maryland, in 1987-88, and worked on the system design of satellite mobile (INMARSAT) communications with the Communication Satellite (COMSAT) Corp., Clarksburg, Maryland, in 1989. From 1989 to 1991, he was with the IBM Thomas J. Watson Research Center, Yorktown Heights, New York to work on high speed wireless LANs. Since September 1991, He has been an associate professor at the Department of Electrical Engineering, National Tsing Hua University, Hsinchu, Taiwan. Dr. Chen is also consulting local and international industrial companies in spread spectrum communication, infrared free space transmission, and wireless protocols. His current research interests include wireless communication and networks, lightwave networks, wideband/multi-media communication, and synchronization.

Dr. Chen was a recipient of the System Research Center Fellowship from 1985 to 1987. He was granted the NSC Class-A research award for 1992 and 1993. He has authored over 40 technical papers in the IEEE journals, documentation and conferences and has couples of U.S. patent applications in process. Dr. Chen has been invited to give talks, short courses, and tutorials regarding wireless communication/networks to academic and industrial research institutions in the U.S., Japan, Europe, Singapore, China. He is a member of IEEE Communication Society Communication Theory, Computer Communication Technical committees, and Personal Communication Committee and has been responsible for organizing and chairing sessions related to wireless networks in major international conferences such as the IEEE ICC, Globecom, Symposium on Personal Indoor Mobile Communication. In addition to being in the editorial board of the International Journal of Wireless Information Networks, Dr. Chen is a voting member of the IEEE 802.11 (an international standard for Wireless LANs) committee.

Chenhsein Lien received his B.S. in Physics from the National Tsing Hua University in 1975 and his Ph.D. in Physics from the Ohio State University in 1982. Since 1983, he has been an associate professor at the Department of Electrical Engineering, National Tsing Hua University, Hsinchu, Taiwan. Dr. Lien is also consulting local industrial companies in electronic devices and circuit design. His current research interests include semiconductor power devices, smart power IC, high speed devices and photonic devices. Dr. Lien was a recipient of the Presidential Fellowship of the Ohio State University for 1982.

Ming-Tang Shih received his B.S. and M.S. in electrical engineering from the National Cheng-Kung University in 1976 and 1978, respectively, and his Ph.D. in EE-Systems from the University of Southern California in 1990. He joined the Electronic Research and Service Organization (ERSO) at the Industrial Technology Research Institute (ITRI) in 1980 working on integrated circuit design for data conversion and telecommunication. Since 1990, Dr. Shih has been with the Computer and Communication Laboratories (CCL) at ITRI, leading a department on transmission signal processing and wireless data communication.

C.-P. Jeremy Tzeng received his B.S. in electrical engineering from National Taiwan University in 1975 and his Ph.D. in EECS from the University of California at Berkeley in 1985. He worked at Rockwell International on integrated circuit design for communications during 1979 to 1982. He joined AT&T Bell Labs. in 1985 working in the areas of communication signal processing, image transmission, and high speed networking. Since 1989, Dr. Tzeng has been with the Computer and Communication Research Laboratories (CCL) at the Industrial Technology Research Institute (ITRI) in Taiwan, as the Director of Communication Technology Division to lead efforts on wireless communications and multimedia signal processing. Dr. Tzeng is the editor of VLSI Communications in the IEEE Transaction on Communications.

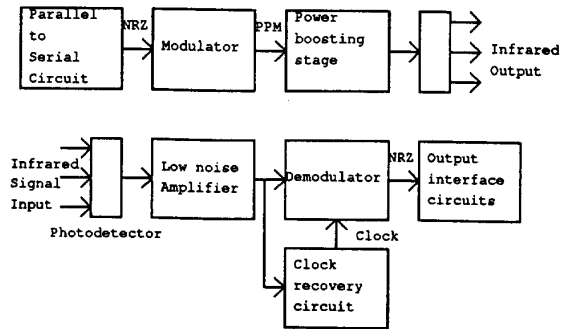


Figure 1: System functional block diagram

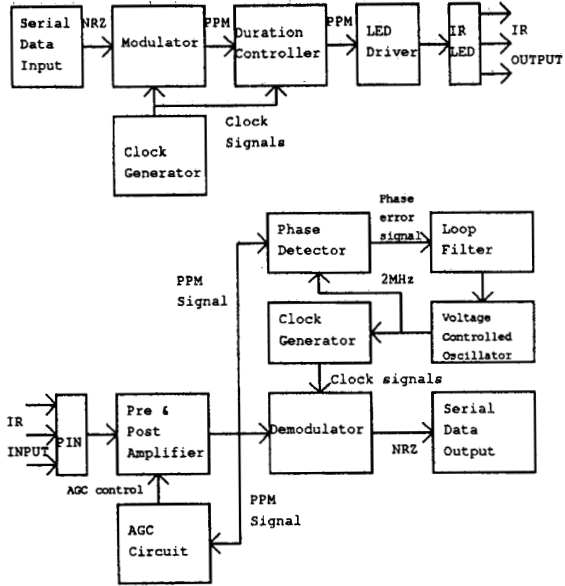


Figure 2: Detailed system block diagram

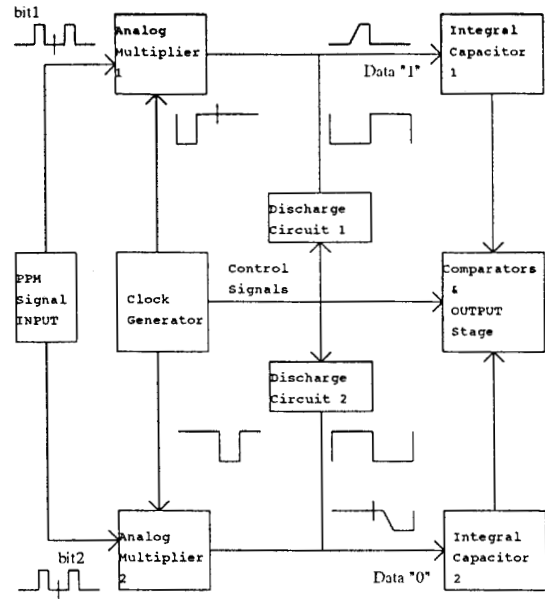


Figure 4: Operation of PPM demodulator

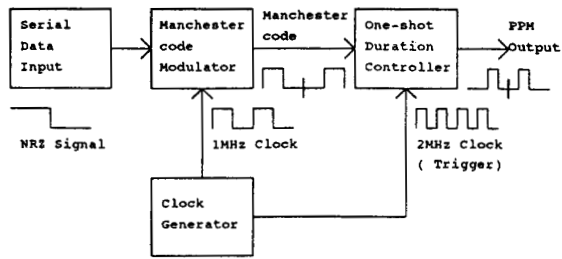


Figure 3: Operation of PPM generating circuit



Figure 5: The output waveform (upper trace, 10 V/div) of the LED driver circuit and the received waveform (bottom trace, 0.2 V/div) from the output of the preamplifier. The horizontal scale is 1 uS/div.

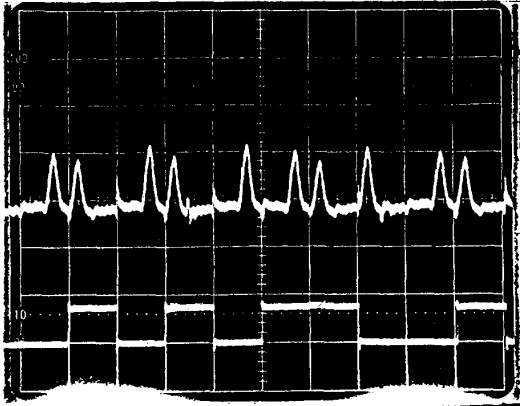


Figure 6: The received waveform (upper trace, 0.2 V/div) from the output of the preamplifier and the output waveform from the demodulator (bottom trace, 5 V/div). The horizontal scale is 1 μ S/div.

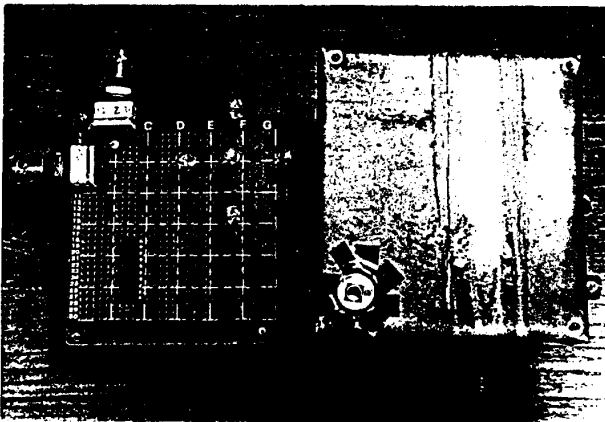


Figure 7: Top view of the transmitter (left) and the receiver (right).